J. Appl. Biol. Chem. **50**(2), 52-57 (2007) **Article**

2D-QSAR and HQSAR on the Inhibition Activity of Protein Tyrosine Phosphatase 1B with Oleanolic Acid Analogues

Young-Ho Chung, Seok-Chan Jang, Sang-Jin Kim[1] and Nack-Do Sung*

Department of Applied Biology & Chemistry, College of Agriculture and Life Sciences, Chungnam National University, Daejeon 305-764, Korea

[1]Department of Cosmetic Science, Daejeon Health Sciences College, Daejeon 300-711, Korea

Received February 7, 2007; Accepted April 6, 2007

Quantitative structure-activity relationships (QSARs) on the inhibition activities by oleanolic acid analogues (1-19) as a potent inhibitor against protein tyrosine phosphatase-1B were studied quantitatively using 2D-QSAR and HQSAR methodologies. The inhibition activity was dependent on the variations of R_4substituent, and as shown in 2D-QSAR model ($r^2 = 0.928$), it has a tendency to increase as the negative Randic Indice (RI) goes up. The size of the molecular fragments used in HQSAR varied from five to eight. The fragment distinctions had the best statistic value, whose predictability is $q^2 = 0.785$ and correlation coefficient is $r^2 = 0.970$, on condition of connections. From the atomic contribution maps, the factor that contributes to the inhibition activities is the C_{15}~C_{17} bond in the D ring. From the analysis result of these two the models, the structural distinctions and descriptors that contribute to the inhibition activities were obtained.

Key words: *2D-QSAR & HQSAR analysis, oleanolic acid analogues, PTP-1B inhibition activity*

PTP composed of many kinds of enzyme makes up a large protein family, and it also dephosphorylates various substrates as an important enzyme of the signal transduction within and between cells. The dephosphorylation of tyrosine is regulated by enzymes, which are protein tyrosine kinase (PTK) that causes phosphorylation, and PTP that induces dephosphorylation. PTP can amplify or reduce the celluar signaling, and hence if the function of PTP is not controlled normally in the human body [Van *et al.*, 1998], the outbreak and progress of disease are accelerated [Zhang, 2001].

Recently, the effect of oleanolic acid on the pigmentation by UV-B irradiation [*Bae et al.*, 2000], as well as those of two terpenoide ursolic acid and oleanolic acid on epidermal permeability barrier and simultaneously on dermal function [Lim *et al.*, 2004] were reported. And 3D-QSAR studies on design and modification [.Black *et al.*, 2005; Larsen *et al.*, 2003; Ala *et al.*, 2006; Hu, 2006] of potent PTP-1B inhibitors [Gyanendra *et al.*, 2006; Zhou *et al.*, 2005; Andersen *et al.*, 2002; Pei *et al.*, 2003; Taha *et al.*, 2005] from natural productors [Liu *et al.*, 2006; Bae *et al.*, 2006; Yang *et al.*, 2006; Na *et al.*, 2006] and potential treatment of diabetes and obesity [Pei *et al.*, 2004] were also discussed and evaluated. In author's previous report, 3D-QSAR [Myung *et al.*, 2005], 2D-QSAR and HQSAR for the inhibition of calcineurin-NFAT signaling by blocking protein-protein interaction with *N*-(4-oxo-1(4H)-naphthalenylidene)benzenesulfonamide analogues were studied [Myung and Sung, 2007]. Also, studies on the CoMFA and CoMSIA on the neuroblocking activity of 1-(6-chloro-3-pyridylmethyl)-2-nitroiminoimidazolidine analogues have been reported [Sung, 2006].

In this study, 2D-QSAR and HQSAR [Lowis, 1997] models were derived between the oleanolic acid analogues and the inhibition activities (IC_{50}) against PTP-1B. From the model, the structural information of substrate derivatives as a PTP-1B inhibitor was acquired.

*Corresponding author
Phone: +82-42-821-6737; Fax +82-32-825-3306
E-mail: ndsung15@hanmail.net

Abbreviations: 2D-QSAR, 2 dimensional quantitative structure-activity relationship; HQSAR, holographic quantitative structure-activity relationship; PTP, protein tyrosine phosphatase; CRC, cyclic redundancy check; PLS, partial least squared; PRESS, predictive residual sum of the square of the training set.

Materials and Methods

Derivation of 2D-QSAR model. The published data was used for the inhibition activity (pI_{50}) of PTP-1B of oleanolic acid (IUPAC: 3β-hydroxy-oleanen-28-oic acid)

from Sansuyu (*Cornus officinalis Sieb.*) and their analogues (**1-19**) [Lihong, 2005; TSAR, 2000] as a substrate molecule. To analyze the structure-activity relation (SAR) among the substrate molecules, the descriptors of R_4-substituents [TSAR, 2000], and the observed inhibition activities (*Obs*.pI_{50}) Hansch-Fujita equation [Fujita *et al.*, 1964] was derived through TSAR program (ver. 3.3) of Oxford Molecular Ltd. and SAS program (ver. 9.1). To have a statistically good model, four chemical compounds (**6, 9, 10 & 11**) that do not contribute to correlativity were selected as outliers, and then the 2D-QSAR model was drawn for training set compounds (n = 15).

Descriptors of substrate molecule. The physicochemical parameters of substrate molecules as a descriptor were calculated using TSAR program (ver. 3.3) and Sybyl program (ver. 7.1). The descriptors used as variables are mass and volume ($Å^2$) of the molecule, surface area ($Å^2$), total lipole, and bond lipole. The hydrophobicity (logP or $\pi_x = logP_x - logP_H$) of substituents and molecules and dipole moment (Debye) were calculated and then used as a descriptor. Besides of these, topological Winer indices and Randic indice were obtained, and the dimensional parameter, molar refractivity (MR: cm^3/mol.) related to the form or size of molecules or substituents was also calculated.

Derivation of HQSAR model. To derive HQSAR model, Sybyl program (ver.7.2) of Tripos was utilized. To obtain a statistically significant model, four chemical compounds, which are **1**, **5**, **13**, and **14**, that do not aid in correlativity were included in the test set. Also, PLS analysis was performed for training set compounds (n = 15) so that the HQSAR model was produced. Above all, to grasp the connection between the size of molecular fragments and the inhibition activity (*Obs*.pI_{50}) surveyed regarding PTP-1B of oleanonic acid derivatives (**1-19**), the fragments were made to become two to ten bin in size, and the length of molecular hologram [Andersen *et al.*, 2002] was selected largely from 53 to 401. At this point, the most favorable result came out in case that the fragment size was seven to ten. At the same condition, the features of the fragments were made to transform so that the HQSAR model would finally render the most statistically significant results. Unique molecular fragments were described in the positive number by CRC [Heritage and Lowis, 1999]. Consequently, by representing the PLS coefficient that calculates the correlativity between the hologram and the organ activities in the atomic contribution map, the information can be acquired regarding reaction points [Chunsheng *et al.*, 2004]. Molecular activities could be also predicted by verifying the type of fragments in relation with compound activities.

PLS analysis. This analysis with Sybyl program (ver.7.2) was utilized to determine the optimum component number for deriving the final HQSAR model using cross-validation. The result of cross-validation is described in cross-validated r^2 (or q^2). Also, from the result of the maximum q^2 and the minimum standard error, the number of components was selected properly. In terms of cross-validation leave one-out (LOO), where the compound is removed one by one from the data set, was used. At this point, when the compatibility is over r^2_{ncv} 0.90, and the predictability is over $r^2_{cv.}$ (q^2) 0.50, the derived models are found to have stability and predictability [Lindber *et al.*, 1988]. Besides, PRESS of the component number was calculated with the observed inhibition activity value and the predicted inhibition activity. In statistics, n indicates the compound number used in regression analysis, r represents the correlation coefficient, r^2 represents the variance in Y explained by the regression, q^2 represents the predictability by cross validation, F represents the ration of the correlation, and s does the standard deviation.

Results and Discussion

Substrate molecules and inhibition activity. Fig. 1 shows oleanolic acid and its structure of derivatives. Table 1 indicates the inhibition activity (*Obs*.pI_{50}) of PTP-1B observed in oleanolic acids, and the predicted inhibition activity (*Pred.* pI_{50}) with 2D-QSAR and HQSAR model. The deviation of two different values was also arranged in Table 1. According to Table 1, the inhibition activity value of PTP-1B was in the range of $pIC_{50} = -1.30 \sim 0.82$. Moreover, while the **3** ($pI_{50} = -1.30$) had the lowest inhibition activity, the **18** ($pI_{50} = 0.82$) had the highest inhibition activity. Accordingly, the inhibition activity in various substituents was dependent on the change of R_4-substituent. Besides, the average deviation value and the PRESS value were found to have approximately a value two times lower. Consequently, the HQSAR was statistically better model than 2D-QSAR.

Analyses of 2D-QSAR model. In Table 2, the weighting

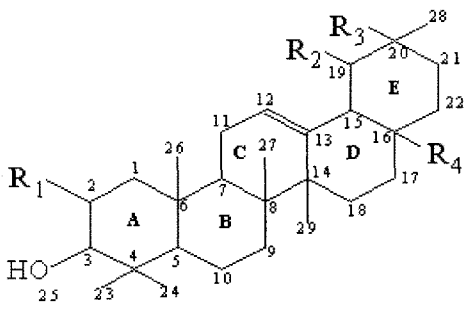

Fig. 1. General structure and numbering scheme of oleanolic acid analogues (1-19) as PTP-1B inhibitor.

Table 1. Observed PTP-1B inhibition activities (*Obs.*pIC_{50}) of oleanolic acid analogues, predicted values (*Pred.*pIC_{50}) by QSAR models and their deviation

No.	Substituents (R)				pIC_{50}	2D-QSAR		HQSAR	
	1	2	3	4		Pred.[a]	Dev.[b]	Pred.[a]	Dev.[b]
1	Me	Me	H	$-CO_2H$	-0.48	-0.45	-0.03	-[d]	-[d]
2[c]	H	H	Me	$-CO_2H$	-0.43	-0.68	0.25	-0.41	-0.02
3	H	H	Me	$-C(=O)NHCH_2CO_2H$	-1.30	-1.15	-0.15	-1.30	0.00
4	H	H	Me	$-C(=O)NH(CH_2)_3CO_2H$	-0.91	-0.70	-0.21	-0.80	-0.11
5	H	H	Me	$-C(=O)NH(CH_2)_{10}CO_2H$	0.17	0.07	0.10	-[d]	-[d]
6	OH	Me	H	$-CO_2H$	-0.46	-[d]	-[d]	-0.43	-0.03
7	OH	Me	Me	$-CO_2H$	-0.41	-0.52	0.11	-0.44	0.03
8	H	H	Me	$-(CH_2)_2CO_2H$	-0.25	-0.24	-0.02	-0.15	-0.10
9	H	H	Me	$-(CH_2)_4CO_2H$	0.04	-[d]	-[d]	-0.26	0.30
10	H	H	Me	$-(CH_2)_8CO_2H$	-0.55	-[d]	-[d]	-0.56	0.01
11	H	H	Me	$-(CH_2)_{12}CO_2H$	-0.75	-[d]	-[d]	-0.66	-0.09
12	H	H	Me	$-C(=O)NHCH(Bz)CO_2H$	0.13	-0.23	0.36	0.16	-0.03
13	H	H	Me	$-C(=O)NHCH(4\text{-}OHBz)CO_2H$	-0.57	-0.40	-0.17	-[d]	-[d]
14	H	H	Me	$-C(=O)NHCH(i\text{-}Pr)CO_2H$	-0.45	-0.37	-0.08	-[d]	-[d]
15	H	H	Me	$-C(=O)NHCH(CO_2H)CH_2CH_2CO_2H$	-1.21	-1.24	0.03	-1.18	-0.03
16	H	H	Me	$-C(=O)NH(4\text{-}CO_2HPh)$	-0.53	-0.47	-0.06	-0.63	0.10
17	H	H	Me	$-C(=O)NH(CH_2)_{10}C(=O)NHCH(Bz)CO_2H$	0.51	0.41	0.10	0.41	0.10
18	H	H	Me	$-(CH_2)_4C(=O)NHCH(Bz)CO_2H$	0.82	0.91	-0.09	0.93	-0.11
19	H	H	Me	$-(CH_2)_3CH(Bz)CO_2H$	0.27	0.44	-0.17	0.28	-0.01
		Ave.[e]					0.13		0.07
		PRESS[f]					0.37		0.16

Abbreviation: Bz = benzyl, i-Pr = iso-propyl, ph = phenyl [a]predicted values by the optimized models, [b]difference between observed value and predicted value, [c]oleanolic acid, [d]outlier or test set compound, [e]average residual of training set, [f]predictive residual sum of squares of the training set.

Table 2. Summary of statistical results and weighting factors in development of 2D-QSAR Model

No.	Intercept	SA	MR	RI	s	F	r^2
1	-2.862	-	0.015	-	2.201	10.09	0.437
2	-4.598	-0.017	0.080	-	1.790	14.59	0.709
3	-3.765	-	0.154	-1.156	1.870	17.09	0.740
4[a]	-5.104	-0.015	0.190	-0.997	1.562	46.90	0.928

Abbreviations: s; mean square, F; F value, r^2; adjust correlation coefficient. SA; surface area (Å^2), MR; molar refractivity (cm^3/mol), RI; Randic index, [a]optimized model & outlier: 4 (**6**, **9**, **10** & **11**), n = 15.

factors of variables contributing to the inhibition activity by every step of 2D-QSAR Model was organized. According to the Table 2, when SA, MR and Randic Indice of molecule were used individually, the correlativity was very low. However, the correlativity ($r^2 = 0.740$) rose slightly more in the case of mixing of MR and RI than the one of MR and SA. Therefore, in the 2D-QSAR model form, **4** that was produced on condition of the mixing of the three variables, had the best correlativity, that is $r^2 = 0.928$.

$$Obs.pI_{50} = -0.997RI(\pm 0.173) + 0.190MR(\pm 0.022) - 0.015SA(\pm 0.003) - 5.104\ (\pm 0.426)$$

$(n = 15, s = 0.162, F = 166.371, q^2 = 0.907$ and $r^2 = 0.928)$

In this form, the coefficient of variables was RI > MR >> SA in order, and RI had the greatest effect on the inhibition activity. In other words, MR and SA had a tiny influence on the inhibition activity. Therefore, the dephosphorylation [Wu and Zhang, 1996], which gets rid of phosphoryl group that cysteine is combined with tyrosine in the catalytic domain, shows that when the negative Randic Indice value of substate molecules is higher, the inhibition activity would increase. The relation

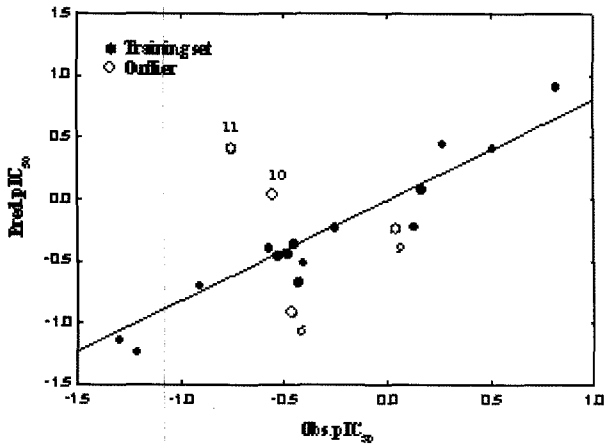

Fig. 2. Relationships between observed inhibition activities (*Obs.*pIC_{50}) and predicted inhibition activities (*Pred.*pIC_{50}) by 2D-QSAR Model I (For training set; *Pred.* pIC_{50}= 0.928*Obs.*pIC_{50}-0.020, n = 15, s = 0.162, F = 166.371, r^2= 0.928 & q^2 = 0.907).

between the observed value of the PTP-1B inhibition activity and the predicted value by 2D-QSAR Model was shown in Fig. 2. By using this form (*Pred.* pIC_{50} = 0.928 *Obs.*pIC_{50}-0.020, n = 15, s = 0.162, F = 166.371, r^2 = 0.928 & q^2 = 0.907) it is believed that the inhibition activity can be predicted.

Analyses of HQSAR model. First, when the size of molecular fragment was five to eight, the most favorable statistic value was obtained, and its result is shown in Table 3. Based on this result Table 4 represents that the model indicating the optimum statistics was searched changing the fragment distinctions by the model that had the optimum statistic value on the condition of the molecular fragment size five to eight. Atoms/bonds, Connections, H-bond donor and H-bond acceptor were used as the fragment distinctions. However, on condition of chirality, the best statistics, which is over q^2 = 0.50 in predictability and over r^2 = 0.900 in correlativity, could not be acquired. Especially, on condition of connections, the optimum model came out, that is q^2 = 0.785 in predictability and r^2 = 0.970 in correlativity. Its length of hologram was 257 bin, and its number of compound was five. Furthermore, the predicted activity value (*Pred.*pIC_{50}) and the observed activity value (*Obs.*pIC_{50}) from the optimum HQSAR model were represented in Fig. 3. From the relation of the linear expression (*Pred.*pIC_{50} = 0.971*Obs.*pIC_{50}-0.011, r^2 = 0.970 & q^2 = 0.956) the high correlativity could be verified between two activity values. Meanwhile, in Table 5, the deviation averages and PRESS values were analyzed regarding the outliers or the test set of each model. As mentioned above, because four compounds that do not contribute to correlativity were eliminated from the training set to derive a statistically significant model, the low predictability is assumed. According to Table 5, the deviation average of both models was analogous to each other. However, 2D-QSAR from PRESS was better model in predictability than HQSAR.

Atomic contribution plots. To compare and analyze

Table 3. HQSAR analyses for the influence of various *fragment sizes* on the key statistical parameters

Models	Fragment size	Best length	$r^2_{cv.}(q^2)$	$SE_{cv.}$	$r^2_{ncv.}$	$SE_{ncv.}$	NC
1	2~5	53	0.425	0.494	0.701	0.356	2
2	3~6	151	0.573	0.492	0.930	0.484	5
3	4~7	257	0.619	0.419	0.949	0.170	5
4[a]	5~8	257	0.785	0.349	0.970	0.131	5
5	6~9	257	0.683	0.424	0.972	0.125	5
6	7~10	61	0.524	0.519	0.956	0.158	5

[a]The best of fragment size, SE_{cv}: cross-validated standard error, $SE_{ncv.}$: non-cross- validated standard error, NC: number of component.

Table 4. HQSAR analyses for various fragment distinction on the key statistical parameters using *fragment size* default (5-8)

Models	Fragment distinctions	Best length	$r^2_{cv.}(q^2)$	$SE_{cv.}$	$r^2_{ncv.}$	$SE_{ncv.}$
4[a]	Connections	257	0.785	0.349	0.970	0.131
4-1	Atoms/bonds[b]	49	0.729	0.392	0.941	0.183
4-2	Donor & Acceptor	353	0.306	0.627	0.925	0.206

[a]The optimized HQSAR model; number of molecules in the training set: 15., number of molecules in the test set: 4 (**1**, **5**, **13** & **14**), [b]In all case, the *atoms* and *bonds* fragment distinction are turned on., SE_{cv}: cross-validated standard error, $SE_{ncv.}$: non-cross-validated standard error, number of component.: 5.

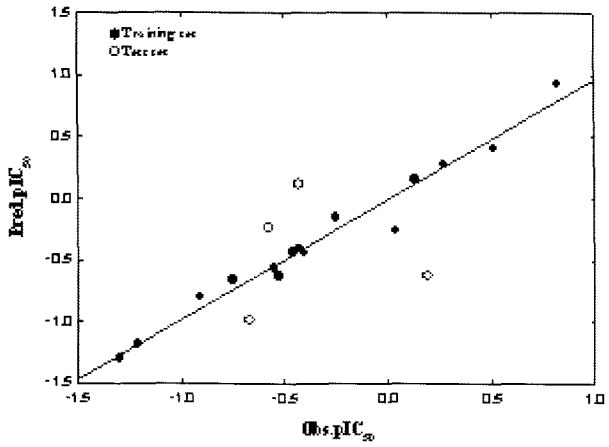

Fig. 3. Relationships between observed inhibition activities (*Obs.*pIC_{50}) and predicted inhibition activities (*Pred.*pIC_{50}) by HQSAR model (IV), (For training set; *Pred.* pIC_{50} = 0.971*Obs.*pIC_{50}-0.011, n = 15, s = 0.108, F = 410.049, r^2 = 0.970 & q^2 = 0.956).

Table 5. Observed inhibition activities, predicted activities (*Pred.*pIC_{50}) by two optimized models and their deviation for the outliers and test set

No.	pIC_{50}[a]	2D-QSAR		No.	HQSAR	
		Pred.[b]	Dev.[c]		Pred.[b]	Dev.[c]
6	-0.46	-0.92	0.46	1	-0.48	-0.29
9	0.04	-0.25	0.29	5	0.68	-0.79
10	-0.55	0.04	-0.59	13	3.74	0.17
11	-0.75	0.40	-1.15	14	2.81	-1.03
Ave.[d]			0.62			0.60

[a]Observed value, [b]predicted values by the optimized QSAR models, [c]different between observed value and predicted value, [d]average residual, [e]predictive residual sum of squares.

the features of substrate compounds that have an effect on the inhibition activity of PTP-1B, the atomic contribution map regarding the **18** of the highest inhibition activity and the lowest one **3**, was shown in Fig. 4. In the map, the green represents the part contributing to activity, and the red represents the non-contributing one. In the structure of the **18** (pIC_{50} = 0.82), the C_1-C_2 and C_3~C_5 bond of A ring, C_{13}~C_{16} bond of D ring, the two methyl groups of E ring, and the methyl group as R_3-substituent aided in the inhibition activity. On the other hand, carboxyl group of R_4-substituent did not help. In the **3** (pIC_{50} = −1.30), which had a low inhibition activity, only the C_{15}~C_{18} bond of D ring did contribute. On the whole, the factor that contributes to the inhibition activities is the C_{15}~C_{17} bond in the D ring. Consequently, in the dephosphorylation process, some parts of the substrate molecules contributed to the inhibition activity, or some parts did not. Therefore, in this study, the information regarding the structural distinctions and the descriptors of the oleanolic acid

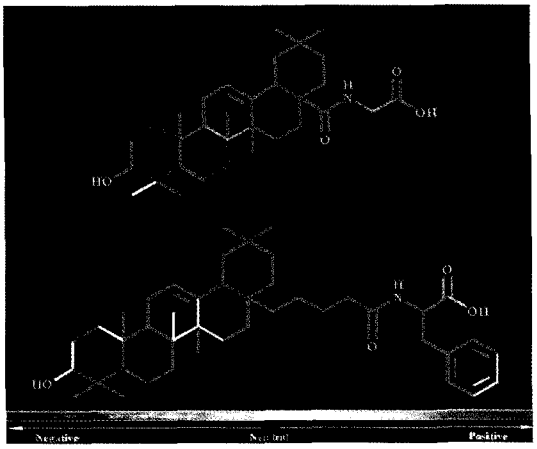

Fig. 4. Atomic contributions maps to the inhibition activities (*Obs.*pIC_{50}) of oleanolic acid derivative (18 = 0.82 & 3 = -1.30): Green color denotes the greatest contribution to the inhibition activity while red color signifies least contribution and gray color signifies average contribution.

derivatives that contribute to the inhibition activity against PTP-1B from the result of 2D-QSAR and HQSAR models was obtained.

Acknowledgments. This work was supported by a grant (No. R11-2002-100-03005) given from ERC program of the Korea Science and Engineering Foundation (KOSEF).

References

Ala PJ, Gonneville L, Hilman M, Milton H, Becker-Pasha M, Yue EW, Douty B, Wayland B, Polam P, Crawley ML, McLaughlin E, Sparks RB, Polam P, Crawley ML, McLaughlin E, Sparks RB, Glass B, Takvorian A, Combs AP, Burn TC, Hollis GF, and Wynn R (2006) Structural insights into the design of nonpeptidic isothiazolidinone-containing inhibitors of phosphatase 1B. *J Biol Chem* **281**, 38013-38021.

Andersen HS, Olsen OH, Iversen LF, Srensen AL, Mortensen SB, Christensen MS, Branner S, Hansen TK, Lau JF, Jeppesen L, Moran EJ, Su J, Bakir F, Judge L, Shahbaz M, Collins T, Vo T, Newman MJ, Ripka WC, and Moller PH (2002) Discovery and SAR of a novel selective and orally bioavailable nonpeptide classical competitive inhibitor class of protein-tyrosine phosphatase 1B. *J Med Chem* **45**, 4443-4459.

Bae JH, Lee WW, Suh KS, and Kim ST (2000) The effect of oleanolic acid and ursodeoxycholic acid on the pigmentation in the mouse by ultraviolet-B (UVB) irradiation. *Korean J Innvestigative dermatology* **7**, 223-229.

Bae EY, Na MK, Njamen D, Mbafor JT, Fomum ZT, Cui L, Choung DH, Kim BY, Oh WK, and Ahn JS (2006) Inhibition of protein tyrosine phosphatase 1B by prenylated isoflavonoids isolated from the sem bark of Eryth-

rina addisoniae. *Planta Medica* **72**, 945-948.

Black E, Breed J, Breeze AL, Embrey K, Garcia R, Gero TW, Godfrey L, Kenny PW, Morley AD, Minsshull CA, Pannifer AD, Read J, Rees A, Russell DJ, Toader D, and Tucker J (2005) Structure-based design of protein tyrosine phosphatase-1B inhibitors. *Bioorg & Med Chem Lett* **15**, 2503-2507.

Chunsheng DC, Xiaodong YW, and Liansheng W (2004) Holographic QSAR of selected esters, *Chemosphere* **57**, 1739-1745.

Fujita T, Iwasa J, and Hansch C (1964). A new substituent constant, π, derived from partition coefficients. *J Am Chem Soc* **86**, 5175-5183.

Gyanendra P and Saxena AK (2006) 3D-QSAR studies on protein tyrosine phosphatase 1B inhibitors: Comparison of the quality and predictivity among 3D-QSAR models obtained from different conformer-based alignments. *J Chem Infor Modeling* **46**, 2579-2590.

Heritage TW and Lowis DR (1999) In *Rational drug design: Novel Methodology and Practical Applications* (ed. Parrill AL, and Reddy MR), Ch. 4., Molecular holo-gram QSAR. ACS Symposium Series 719, *ACS.* Wash-ington, DC.

Hu X (2006) In silico modeling protein tyrosine phos-phatase-1B inhibitors with cellular activity. *Bioorg Med Chem Lett* **16**, 6321-6327.

Larsen SD, Stevens FC, Lindberg TJ, Bondnar PM, O'Sulli-van TJ, Schostarez HJ, Palazuk BJ, and Bleasdal JE (2003) Modification of the N-terminus of peptidomi-metic protein tyrosine phosphatase 1B (PTP1B) inhibi-tors: Identification of analogues with cellular activity. *Bioorg Med Chem Lett* **13**, 971-975.

Lihong H (2005) Triterpenoic acid derivatives as protein tyrosine phosphatase-1B inhibitors, 031505201(CH), PCT/CN2005/000172 (PCT).

Lihong H (2005) Drug Discovery Based on Traditional Chi-nese Medicine. In *Proceedings of International Sympo-sium on Development of Chinese Cosmetic Technology.* Autumn. *The Society of Cosmetic Sciencetists of Korea.* **31**, 3-30.

Lim SW, Jung SW, and Ahn SK (2004) The effect two ter-penoide ursolic acid and oleanolic acid on epidermal permeabitiy barrier and simultaneously on dermal func-tion. *J Soc Cosmet Scientisis korea* **30**, 263-278.

Lindber W, Persson JA, and Wold S (1988) Partial lesast-squares method for spectrofluorimetric analysis of mix-ture of humic acid and ligninsulfonate. *Anal Chem* **55**, 643-648.

Liu Q, Xu H, Zhang T, Fan X, and Han L (2006) A new compound as PTP 1B inhibitor from the red alga polysi-phonia urceolata. *Huaxue Tongbao* **69**, 708-710.

Lowis DR (1997) In *HQSAR. A new, highly prediction QSAR technique.* Tripos Technical Notes. **1**, No. 5.

Myung PK, Park KY, and Sung ND (2005) CoMFA and CoMSIA on the inhibition of calcineurin-NFAT signal-ing by blocking protein-protein interaction with *N*-(4-oxo-1(4H)-naphth-alenylidene)benzenesulfonamide deriv-atives. *Bull Korean Chem Soc* **26**, 1941-1945.

Myung PK and Sung ND (2007) 2D-QSAR and HQSAR for the inhibition of calcineurin-NFAT signaling by blocking protein-protein interaction with *N*-(4-oxo-1(4H)-naphthalenylidene)benzenesulfonamide analogues. *Arch Pharm Res* **30**, In press.

Na MK, Jang JP, Njamen D, Mbafor JT, Fomum ZT, Kim BY, Oh WK, and Ahn JS (2006) Protein tyrosine phos-phatase-1B inhibition activity of isoprenylated fla-vonoids isolated from Erythrina mildbraedii. *J Natural Prod* **69**, 1572-1576.

Pei Z, Li X, Liu G, Abad-Zapatero C, Lubben T, Zhang T, Ballaron SJ, Hutchins CW, Trevillyan JM, and Jirousek MR (2003) Discovery and SAR of novel, potent and selective protein tyrosine phosphatase-1B inhibitors. *Bioorg & Med Chem Lett* **13**, 3129-3132.

Pei Z, Li X, Lubben TH, and Szezepankiewicz BG (2004) Inhibition of protein tyrosine phosphatase 1B as a poten-tial trearment of diabetes and obesity. *Curr Pharm Design* **10**, 3481-3504.

Sung ND, Jang SC, and Choi KS (2006) CoMFA and CoMSIA on the neuroblocking activity of 1-(6-chloro-3-pyridylmethyl)-2-nitroiminoimidazolidine analogues. *Bull Korean Chem Soc* **27**, 1741-1746.

Taha MO and AlDamen MA (2005) Effects of variables docking conditions and scoring functions on correspond-ing protein-aligned comparative molecular similarity indices analysis models constructed from diverse human protein tyrosine phosphatase 1B inhibitors. *J Med Chem* **48**, 8016-8034.

TSAR (2000) Proprietary Software (Ver. 3.3), Oxford Molecular Ltd..

Van Vactor D, Reilly AM, and Neel BG (1998) Genetic analysis of protein tyrosine phosphatases. *Curr Opin Genet Dev* **8**, 112-126.

Wu L and Zhang ZY (1996) Probing the function of the Asp128 in the lowe molecular weight protein tyrosine phosphatase-catalyzed reaction A presteadystate and steady state kinetic investigation. *Biochemistry* **35**, 5426-5434.

Yang S, Na MK, Jang JP, Kim KA, Kim BY, Sung NJ, Oh WK, and Ahn JS (2006) Inhibition of protein tyrosine phosphatase 1B by lignans from Myristica fragrans. *Phy-totherapy Res* **20**, 680-682.

Zhang ZY (2001) Protein tyrosine phosphatases: prospects for yherapeutics. *Curr Opin Chem Biol* **5**, 416-423.

Zhou M and Ji M (2005) Molecular docking and 3D-QSAR on 2-(oxalylamino)benzoic acid and its analogues as pro-tein tyrosine phosphatse 1B inhibitors. *Bioorg & Med Chem Lett* **15**, 5521-5525.